

ACCEPTED MANUSCRIPT • OPEN ACCESS

## Generation of high-energy soliton-like pulses in 1.9-2.5 $\mu\text{m}$ spectral domain

To cite this article before publication: Vladislav Dvoyrin *et al* 2020 *J. Phys. Photonics* in press <https://doi.org/10.1088/2515-7647/abb585>

### Manuscript version: Accepted Manuscript

Accepted Manuscript is “the version of the article accepted for publication including all changes made as a result of the peer review process, and which may also include the addition to the article by IOP Publishing of a header, an article ID, a cover sheet and/or an ‘Accepted Manuscript’ watermark, but excluding any other editing, typesetting or other changes made by IOP Publishing and/or its licensors”

This Accepted Manuscript is © 2020 The Author(s). Published by IOP Publishing Ltd.

As the Version of Record of this article is going to be / has been published on a gold open access basis under a CC BY 3.0 licence, this Accepted Manuscript is available for reuse under a CC BY 3.0 licence immediately.

Everyone is permitted to use all or part of the original content in this article, provided that they adhere to all the terms of the licence <https://creativecommons.org/licenses/by/3.0>

Although reasonable endeavours have been taken to obtain all necessary permissions from third parties to include their copyrighted content within this article, their full citation and copyright line may not be present in this Accepted Manuscript version. Before using any content from this article, please refer to the Version of Record on IOPscience once published for full citation and copyright details, as permissions may be required. All third party content is fully copyright protected and is not published on a gold open access basis under a CC BY licence, unless that is specifically stated in the figure caption in the Version of Record.

View the [article online](#) for updates and enhancements.

# Generation of High-Energy Soliton-Like Pulses in 1.9-2.5 $\mu\text{m}$ Spectral Domain

Vladislav V. Dvoyrin\* and Sergei K. Turitsyn

*Aston Institute of Photonic Technologies, Aston University, Birmingham B4 7ET, UK.*

*Aston-Novosibirsk International Centre for Photonics, Novosibirsk State University,*

*Novosibirsk 630090, Russia.*

\*v.dvoyrin@ston.ac.uk

**Abstract:** We experimentally demonstrate the generation of soliton-like pulses with 195-230 fs duration and energy up to 20 nJ in the spectral region of 1.9-2.5  $\mu\text{m}$  directly from the Tm-doped all-fiber MOPA laser. The emerged Raman solitons generated directly in the fiber amplifier exhibit unusual dynamics and spectral properties forming a supercontinuum without conventional gaps between Stokes pulses. Namely, at the output powers above 2W, in addition to conventional soliton spectral peaks beyond 2.3  $\mu\text{m}$ , we observe high spectral density over an extended range of 1.95-2.23  $\mu\text{m}$  corresponding to a coherent structure that to the best of our knowledge differs from any previously observed supercontinuum regimes. The average optical power of the fiber laser is at 3-W level, whereas the estimated peak power reached 80-kW level. Such a relatively simple laser system with high spectral density is a promising light source for various applications ranging from advanced comb spectroscopy to ultra-fast photonics.

**Keywords:** Mode-locked Fiber Lasers, Fiber Amplifiers, Solitons, Optical Supercontinuum.

## 1. Introduction

Conventional optical fibers have anomalous dispersion at wavelengths higher than approximately 1.3  $\mu\text{m}$ . Nonlinear propagation of light in fiber waveguides in the main order is governed by the nonlinear Schrödinger equation (NLSE) [1], which in the case of the anomalous dispersion has well-known solutions in the form of localized coherent pulses - solitons (see, e.g. [1-3] and references therein). A powerful enough initial waveforms of arbitrary shape (including CW radiation, as an ultimate case) during propagation down the fiber tend to transform, eventually, into soliton or set of solitons [1-3]. From a practical viewpoint, solitons have many attractive features, such as remarkable stability, a uniform phase across the pulse, and well-defined properties, e.g. pulse energy is inversely proportional to the soliton width. However, at the same time, they possess certain drawbacks, for instance, the energy of the fundamental soliton generated in the laser resonators is limited by the so-called Kelly sidebands [4]. In the case of the normal fiber dispersion it is possible to generate dissipative solitons (see e.g. [5-7] and reference therein) that can offer higher pulse energies compared to conventional solitons. However, in the red part of the spectrum (longer wavelengths), use of the normal dispersion in fibers is technical challenging.

Note, that an accurate description of the propagation of powerful and spectrally broad radiation goes beyond the NLSE model with Raman and higher-order dispersion both affecting formation of short enough pulses. Moreover, even in the limit of pure NLSE model nonstationary solutions (varying along the fiber) can be used to generate at the output new types of localized pulse with a broad spectrum. Exploration of new forms of pulses and complex coherent structures supported by optical fibers is both an interesting scientific and an important practical problem. Of a special interest is generation of structures coherent over ultra-wide spectral interval. For instance, comb spectroscopy is based on availability of a coherent optical supercontinuum (SC) source [8, 9]. Supercontinuum can be produced in the highly nonlinear fibers through spectral broadening based on a four-wave-mixing process

1  
2  
3 characterized, in general, by generation of numerous temporal structures and de-phasing of  
4 spectral components. Even when SC consists of a set of individual solitons their relative  
5 phases might be randomly distributed (due to the underlying pseudo-random four-wave-  
6 mixing dynamics), leading in the limit of many pulses to interesting optical phenomenon -  
7 soliton gas [10]. Typically, such SC is incoherent or quasi-coherent [8, 9] and, therefore, is not  
8 optimal for applications in the comb spectroscopy. Therefore, study of new nonlinear  
9 mechanisms leading to formation of coherent, spectrally broad structures are of high practical  
10 interest. Here we consider approach based on the exploiting Raman effect in an optical fiber  
11 amplifier.

12 Conventional applications of the Raman effect are based on the complete or almost  
13 complete transfer of energy from pump in the shorter wavelength (blue) part of the spectrum  
14 to the longer wavelengths (red part). Thus, energy is shifting from blue part to the red. This  
15 conventional process leads to visible spectral gaps between forming Stokes pulses. Such gaps  
16 are undesirable for many supercontinuum applications. In this work, we explore a possibility  
17 to arrange a continuous energy cascade from blue to red part of the spectrum, while keeping  
18 blue part at the target level of spectral power by constant pumping in this region. This  
19 provides an opportunity to generate temporally short coherent structures with high spectral  
20 density.

21 A laser producing a single spectrally broadband intensive optical pulse would be highly  
22 attractive for spectral comb application. Moreover, lasers generating ultrashort broadband  
23 pulses in the mid-IR range beyond 2  $\mu\text{m}$ , in particular, in the atmospheric transparency  
24 window in between 2 and 2.5  $\mu\text{m}$ , are in special demand due to various practical applications.  
25 Highly intensive optical pulses are required for various applications, including  
26 micromachining and modification of material properties like inscribing of waveguides [11],  
27 LIDAR systems [12], optical coherence tomography [13], trace gas sensing [14] and others.

28 Tm-doped ultrafast fiber laser already overcame 100-W and 200-MW levels in average  
29 and peak powers, respectively [15, 16]; tens- and hundreds-millijoules pulse energies were  
30 demonstrated [16, 17]. Such noticeable results were obtained with bulk optics in master  
31 oscillator – power amplifier (MOPA) systems. Generation of broadband optical pulses (~1.85-  
32 2.05  $\mu\text{m}$ ) directly in the oscillator was also reported [18], as well as generation of spectrally  
33 tunable (1.93-2.2  $\mu\text{m}$ ) coherent Raman solitons in fiber amplifier [19]. However, the output  
34 average power of the fiber oscillator producing broadband pulses [18] was 20 mW, leaving  
35 room for potential further improvement, that we explore in this work. A high-power SC  
36 generation in this spectral range was demonstrated by several methods, for instance, pumping  
37 of a Ho-doped fiber amplifier with intense 1.6- $\mu\text{m}$  Q-switched pulses [20], amplification of  
38 microseconds pulses from gain-switched and mode-locked Tm/Ho-doped laser in a Tm-doped  
39 amplifier [21, 22], amplification of SC generated with mode-locked or nanosecond Er-doped  
40 fiber lasers in Tm- or Tm/Ho-doped fiber amplifiers [23-29]. Generation of 25-W SC  
41 spanning from 2 to 2.5  $\mu\text{m}$  has been demonstrated for a silica-based Tm-doped fibre amplifier  
42 seeded with SC produced in the result of break-up of nanosecond pulses at 1.5  $\mu\text{m}$  [30].  
43 Pumping a specialty high-NA normal-dispersion silica fiber by Tm-doped MOPA fiber laser  
44 resulted in SC spanning from 1.77 to 2.33  $\mu\text{m}$  with 92 mW of output power [31].

45 Generation of spectrally tunable Raman solitons and high-power mid-IR optical SC  
46 directly in straightforward all-fiber Tm-doped MOPA fiber lasers is a powerful tool for  
47 producing pulses with a substantially higher intensity and shorter duration compared to the  
48 "parent" pulse of a seed laser [32-34]. In this work, we present new results on application of  
49 this promising approach. We observed unusual dynamics of Raman solitons generated directly  
50 in the fiber amplifier that results into formation of a supercontinuum without characteristic  
51 gaps between conventional Stokes pulses. Namely, we observe, for the first time, to the best  
52 of our knowledge, a soliton-like structure with a high spectral density over an extended range  
53 of 1.95-2.23  $\mu\text{m}$ . This process allows to increase the pulse energy through the spectral  
54 broadening, in which Raman effect transfers power to the longer wavelengths and the  
55  
56  
57  
58  
59  
60

pumping wave compensates this migration by new portion of incoming power without exhaustion of the shorter wavelength region. We demonstrate this new phenomenon using a relatively simple setup that makes this technique potentially promising for generation of high-power single-pulse optical supercontinuum highly demanded for various spectroscopic applications including advanced comb spectroscopy.

## 2. Methods

An all-fiber core-pumped linear-cavity SESAM-mode-locked Tm-doped silica fiber laser assembled similar to [32] is used as a pump source. The seed laser pumped by a laser diode at the wavelength of 1560 nm operates at the wavelengths of 1925 nm (Fig. 1a) with the full width at half maximum (FWHM) of 3.4 nm; the pulse duration of the seed laser is about 2 ps with the repetition rate of 69 MHz; the average output power is about 3.5 mW. The typical pulse trains observed from the seed laser and amplifier are shown in Fig. 1b.

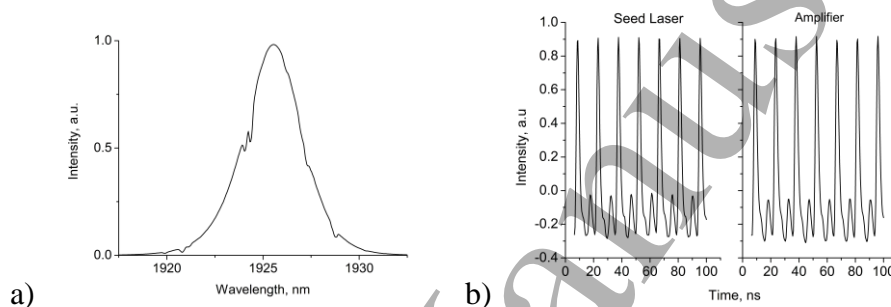


Fig. 1. Optical spectrum of the seed laser (a), and typical pulse trains (b). (The smaller pulses are artefacts of measurement representing detector's response function.)

The fiber amplifier shown in Fig. 2 is based on a 4-m length span of a commercially available silica-based Tm-doped double-clad fiber (DCF-TM-12/128P, CorActive High-Tech Inc.). Its core and clad diameters amount to 12 and 130  $\mu\text{m}$ , respectively, and its cladding cross-section is octagonal. The amplifier is clad-pumped in a forward direction by a laser diode operated at the wavelength of 793 nm. The cladding of the angle-cleaved 0.5-m span of the single-mode passive fiber (SM-2000, Thorlabs, Inc.) spliced with the amplifier output does not guide light, and the laser emission, consequently, does not contain unabsorbed pump radiation.

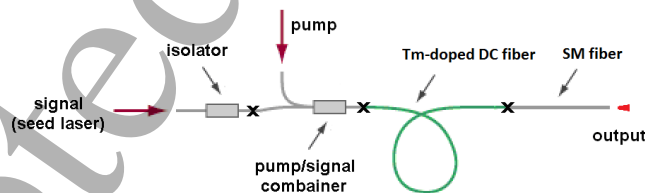


Fig. 2. Scheme of the amplifier.

Pulse trains are recorded with an optical semiconductor detector (extended InGaAs) with 1-ns response time. Optical spectra have been observed with an optical spectrum analyzer in the wavelength domain. For readers' convenience, the frequency scale is also shown in figures representing the spectra. Power fraction corresponding to specific spectral components was calculated from the optical spectra using the knowledge about the total output optical power measured with a thermal power meter.

The interferometric autocorrelations traces were recorded with a home-made autocorrelator built using the Michelson interferometer scheme. Si or InGaAs optical detectors

operating in two-photon absorption mode have been used for the detection of the autocorrelation traces. The intensity autocorrelations have been numerically restored using Fourier-filtering. The pulse durations have been calculated from the intensity autocorrelation traces under the assumption of the pulses' sech<sup>2</sup>-profile.

### 3. Results

#### 3.1 Raman Solitons: Optical Spectra

Raman solitons have been generated directly in the amplifier. At approximately 450 mW of the total output power, a formation of a typical Raman soliton [14] was observed in the output spectra, see Fig. 3. The soliton holds 84% of the total energy. With pump power increase, its Raman frequency self-shift (RFSS) was observed along with the formation of an additional Raman soliton. The part of the total energy stored in the primary Raman soliton started to decrease after the formation of the second one. The average power corresponding to the first Raman soliton, however, increased reaching its maximum of 550 mW when the soliton spectral position shifted to 2.2  $\mu\text{m}$  as shown in Fig. 3.

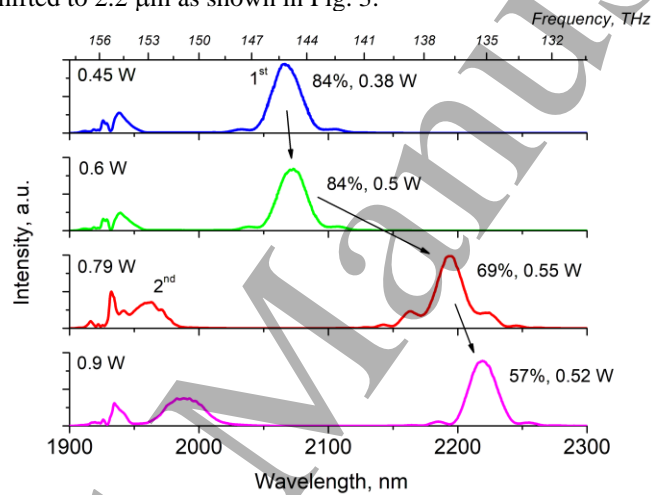


Fig. 3. Output spectra for the output powers of 0.45, 0.59, 0.79, and 0.9 W.

The spectral FWHM of the 1<sup>st</sup> Raman soliton experiencing RSFSS remained nearly constant consisting of 25 nm (1.75 THz). The side-lobes became more pronounced at higher output powers due to increased excessive energy of the soliton.

The FWHM spectrum of the 2<sup>nd</sup> Raman soliton centered near 2  $\mu\text{m}$  amounted to 35 nm (2.6 THz) and was continuously rising in magnitude to  $\sim 70$  nm ( $\sim 4.5$  THz), when the soliton shifted to 2.2  $\mu\text{m}$ , as illustrated by Fig. 4. Its spectral shape experienced deformation during RFSS; therefore, this pulse is referred as the 2<sup>nd</sup> soliton-like pulse in what follows. Near 2  $\mu\text{m}$ , the 2<sup>nd</sup> soliton-like pulse had a longer red wing. At around 2.15  $\mu\text{m}$  it acquired an almost symmetrical shape. But near 2.2  $\mu\text{m}$  (Fig. 5) it again distorted so that the blue wing became stronger. Simultaneously, the formation of the 3<sup>rd</sup> soliton-like pulse was noticed in the spectrum.

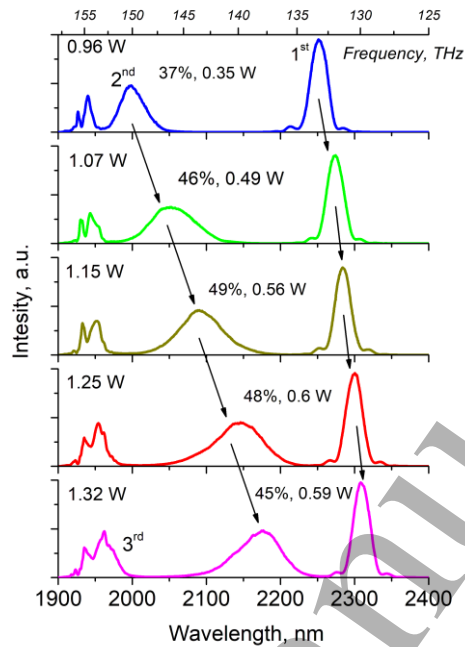


Fig. 4. Output spectra for the output powers of 0.96, 1.07, 1.15, 1.25 and 1.32 W.

At the higher output power (see Fig. 5), RFSS of the 2<sup>nd</sup> soliton-like pulse was noticeably weaker. It took the symmetrical sech<sup>2</sup> shape at 1.52 W, when its spectral maximum passed 2.2  $\mu\text{m}$ . Its FWHM (equal to 37 nm or 2.25 THz at 1.52 W of output power) almost returned to the initial magnitude of 35 nm. The 1<sup>st</sup> Raman soliton spectral position, FWHM, and pulse energy changed insignificantly. The 3<sup>rd</sup> soliton-like pulse distinctly separated from the parent pulse.

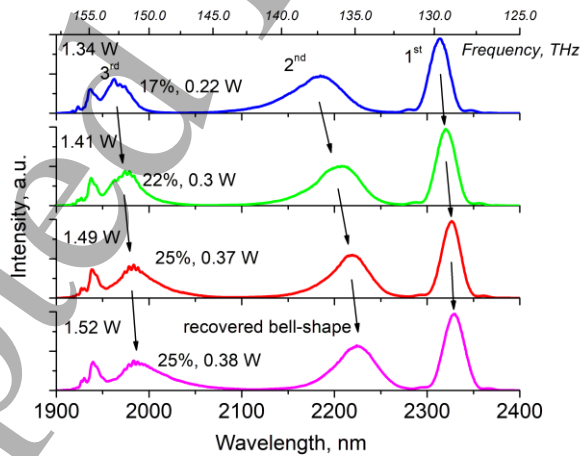


Fig. 5. Output spectra for the output powers of 1.34, 1.41, 1.49, and 1.52 W.

Beyond 2.2  $\mu\text{m}$ , the 2<sup>nd</sup> soliton-like pulse had the characteristic symmetric soliton-like shape (Fig. 6). At the same time, the changes in the parameters of the 1<sup>st</sup> Raman soliton were negligible. The 2<sup>nd</sup> soliton-like pulse experienced a stronger RFSS, and eventually both pulses noticeably overlapped in the spectral domain.

The specific spectral evolution was more pronounced for the 3<sup>rd</sup> soliton-like pulse: it had an asymmetric shape and its spectral shift was accompanied by the rise of its "red" wing. In the vicinity of 2.2  $\mu\text{m}$ , however, its "blue" wing became stronger.

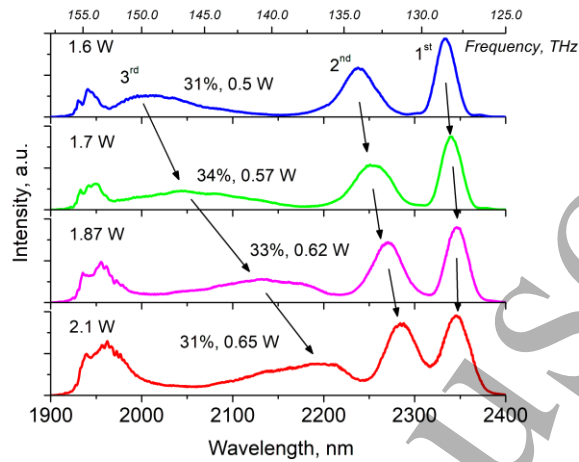


Fig. 6. Output spectra for the output powers of 1.6, 1.7, 1.87, and 2.1 W.

At the output power of 1.7 W, approximately, a formation of another spectral structure in the vicinity of the parent pulse was observed. Its evolution was rather different from that one expected for conventional Raman solitons experiencing RFSS. This was manifested as the strong rise of the red wing and a very weak shift of the spectral maximum. The asymmetric shape of this structure was well pronounced. At higher output powers, see Fig. 7, the rise of its red wing led to the formation of a continuous flat spectral profile, i.e. an optical supercontinuum. By analogy with the formation of the previous soliton-like pulses, we suppose that the whole spectral area shown in dashed box in the Fig. 7 can be mainly attributed to a femtosecond-scale pulse, which represents the main result of our work.

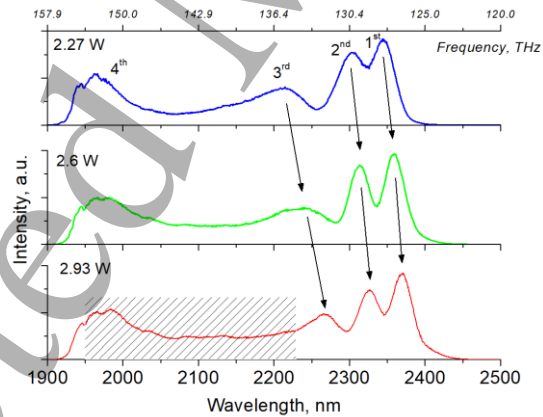


Fig. 7. Output spectra for the output powers of 2.27, 2.6, and 2.93 W. The presumable area of the 4<sup>th</sup> Raman soliton at 2.93 W of the output power is hatched.

The FWHM of the 3<sup>rd</sup> soliton-like pulse centered at 2.29  $\mu\text{m}$  at the highest output power was estimated from spectra after deduction of the spectral pedestal. It was found to be equal to approximately 40 nm (2.3 THz), i.e. comparable to other solitons. The conclusions made from the spectral analysis are supported by study of the autocorrelation traces, which is provided in the next section.

### 3.2 Raman Solitons: Autocorrelation Traces, Si detector

The autocorrelation traces have been studied neglecting the presence of the parent pulse due to its low intensity. The Si detector has a cut-off at approximately 1100 nm. The autocorrelator operated in two-photon absorption mode. Therefore, the impact of the radiation above  $\sim 2.2 \mu\text{m}$  was negligible, and it was possible to observe the autocorrelation trace of each soliton-like pulse separately, when other pulses did not exist or existed at wavelengths longer than  $2.2 \mu\text{m}$ . The intensity autocorrelation traces of the pulses were well approximated by the  $\text{sech}^2$  profile. Both interferometric and intensity autocorrelation traces of the soliton-like pulses are shown in Fig. 8. The traces corresponding to the 1<sup>st</sup> Raman soliton are presented in Fig. 8a. The FWHM of the intensity autocorrelation was equal to 300 fs. Under the assumption of the  $\text{sech}^2$  soliton temporal profile, the pulse duration amounted to 195 fs, which almost corresponded to the time-bandwidth limit of 190 fs. The pulse energy evaluation of 7.2 nJ from the spectra gives an estimate of the pulse peak power above 30-kW level.

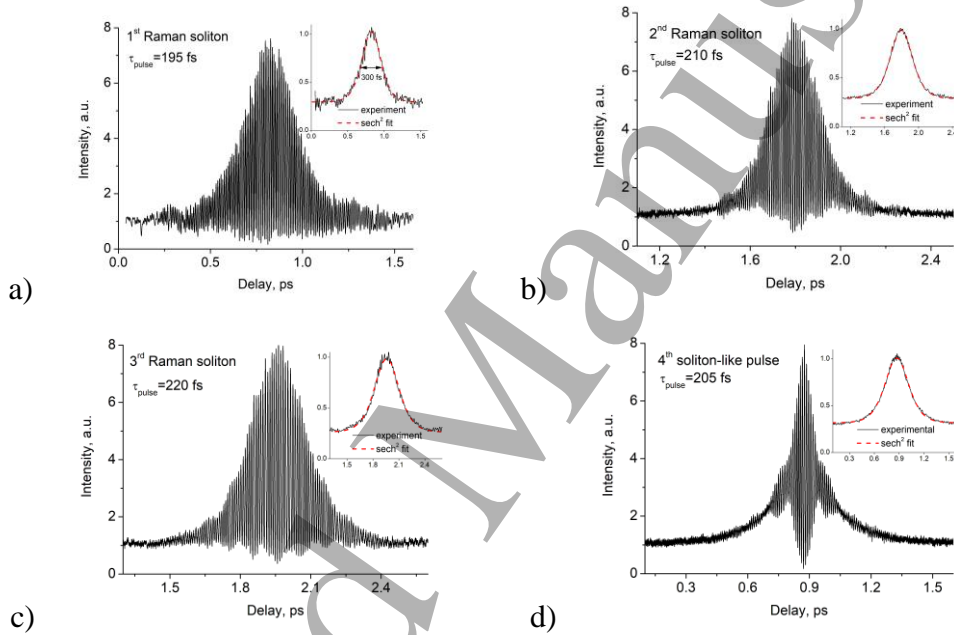


Fig. 8. Interferometric and intensity autocorrelations observed at the output powers of 0.6 (a), 1.25 (b), 1.49 (c), and 2.93 (d) W.

The duration of the 2<sup>nd</sup> soliton-like pulse at the output power of 1.25 W is estimated as 210 fs. This magnitude was greater than the time-bandwidth limit of  $\sim 70$  fs calculated for the FWHM of 72 nm (4.65 THz) and the minimum time-bandwidth product for  $\text{sech}^2$ -shape of 0.315. Its spectral shape was asymmetric, and the interferometric autocorrelation, Fig. 8b, corresponds to the typical shape of a chirped pulse. Its peak power estimated in the mentioned above way reached 35-kW level.

The 3<sup>rd</sup> soliton-like pulse duration calculated for the output power of 1.49 W was about 220 fs being of the same magnitude as the other pulses although its asymmetric spectrum at this power was narrower, its FWHM was equal to 40 nm (3 THz). This is apparently the manifestation of a smaller chirp, which can be qualitatively observed when comparing Fig. 8, b and c. The peak power of this soliton is at the lower level of 20 kW. As this autocorrelation trace corresponds to the beginning of the pulse spectral evolution, for its energy of 5.3 nJ, greater peak power is expected at higher output powers and higher pulse energies.



Finally, the autocorrelation traces of the 4<sup>th</sup> soliton-like pulse (see Fig. 8d) recorded at the output power of 2.93 W is well approximated by a  $\text{sech}^2$  curve, too, indicating probably that the pulse shape in the time-domain has solitonic nature, despite of the fact that its spectral shape is a conventional symmetric  $\text{sech}^2$  shape. This regime, certainly, needs further study. The autocorrelation trace of this pulse resembles typical traces of strongly chirped pulses [35–37]. The duration of this pulse obtained from the autocorrelation trace was equal to 205 fs. Because the spectral components of the pulse beyond 2.2  $\mu\text{m}$  were filtered out, the pulse energy is estimated by the integration in the spectral range of 1.95–2.2  $\mu\text{m}$  that gives the pulse energy estimate of 18 nJ and the corresponding peak power of 77 kW – i.e. 80-kW peak power level.

### 3.3 Raman Solitons: Autocorrelation Traces, InGaAs detector

Evidently, due to simultaneous detection of several pulses with the InGaAs detector, such traces did not allow to characterize a single pulse. However, the 4<sup>th</sup> soliton-like pulse at high output powers became noticeably stronger than others, and, we can assume that it should dominate the trace. Indeed, the intensity autocorrelation trace at the output power of 2.93 W shown in Fig. 9 resembles this one obtained with Si detector.

This autocorrelation trace was broader than the result recorded at the same output power with the Si detector, and the pulse duration amounted to 230 fs, which is longer than durations of other pulses obtained with Si detector. It is supposed that the spectral filtering of the strongly chirped pulse by the Si detector decreased its duration by cutting its red spectral components (back-front in time-domain). Thus, the results obtained with InGaAs detector are believed to more adequately reflect the 4<sup>th</sup> soliton-like pulse duration. However, evidently, further more detailed studies of the fine nature of this pulse are required.

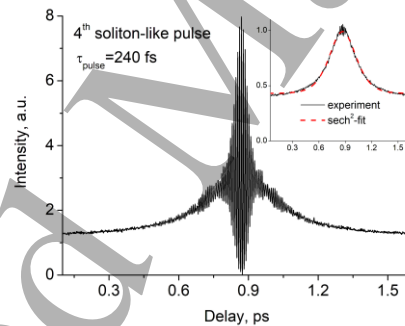


Fig. 9. Interferometric and intensity autocorrelations recorded with the InGaAs detector at the output power of 2.93 W.

The pulse energy can be estimated by cutting the spectral parts, in which other pulses (including the remains of the parent pulse) are distinctly visible. The power fraction for such region of 1.95–2.25  $\mu\text{m}$  (Fig. 7, hatched area) corresponds to 48% of the total emission. This allows us to estimate the average power as 1.38 W, and the pulse energy as 20 nJ, which corresponds to 77 kW for a 230-fs pulse, or to the 80-kW peak power level. This estimate shows that the pulse peak power was noticeably greater as compared to other pulses.

### 3.4 Energetic aspects

The dependence of the output power on the launched pump power is shown in Fig. 10. The maximum output power reached 2.93 W at approximately 23 W of the pump power. The amplifier slope efficiency consisted of 18%.

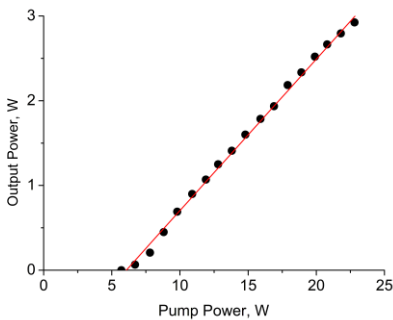


Fig. 10. Output amplifier power vs. pump power.

The maximum pulse energies are estimated from the spectra for the region of 2-2.3  $\mu\text{m}$ . The maximum energy of the 1<sup>st</sup> Raman soliton consists of 8 nJ. The 2<sup>nd</sup> soliton-like pulse maximum energy was found to be higher, about 8.7 nJ. The 3<sup>rd</sup> soliton-like pulse maximum energy estimation was greater corresponding to 9.4 nJ. The already estimated last pulse energy is about 20 nJ. This pulse covered  $\sim 300\text{-nm}$  spectral area, and its spectrum flatness amounted to 3.6 dB in the assumption that the peaks at  $>2.25 \mu\text{m}$  belonged to other pulses. The minimum spectral power density was more than 3.5 mW/nm in the whole spectral range. Thus, this pulse represents itself as a good optical supercontinuum.

#### 4. Discussion

As it has been shown in [32], in the process of soliton compression the parent pulse breaks up into several spikes giving rise to an ultrashort Raman soliton experiencing the RFSS due to its high peak power. The other pulses elongate forming eventually a long-lasting smooth pedestal. After break-up of the parent pulse, the Raman soliton typically stores about a half of the total energy. In this work, we intentionally shifted the laser wavelength at 1925 nm and used co-propagating pump scheme in order to increase re-absorption of the remaining parent pulse. Therefore, it was possible to transfer 84% of total output optical power into the newborn Raman soliton, as it is seen in Fig. 3. Strong suppression of the parent pulse in the amplifier output simplified the pattern of the autocorrelation traces eliminating multi-pulsing dynamics. This enabled analysis of the complex picture of the pulse evolution with increase the pump power of the amplifier. From the practical viewpoint, this approach will allow development of relatively simple fiber laser source emitting ultrashort Raman solitons with a high spectral purity. The remaining fraction of the short-wavelength components can be responsible for such features of the interferometric autocorrelation traces as the non-zero minimum intensity and deviation from 1:8 of the ratio of the maximum intensity to the background. These effects exist for some traces shown in Fig. 8 and 9, and presumably can be explained by the presence of the short-wavelength components incoherent with the most intense pulse.

Investigation of autocorrelations of optical supercontinua have been already reported (see e.g. [38-40] and references therein). Typically, autocorrelation traces are represented by a rather complicated structure with a broad pedestal [38-41], something that has not been observed in the present experiments. We attribute this to suppression of the contributions that affect coherence by reabsorption of corresponding spectral components in the active fiber. Spectral filtering of the optical supercontinuum allowed to reveal autocorrelation trace of its constituents (Raman solitons) [42]. However, a detailed analysis of supercontinuum structure is presented mainly by numerical simulations, e.g. [8]. The Raman solitons in our experiment are well-resolved in optical spectra, and the observed autocorrelation traces are not strongly chirped except for the last soliton-like component. Note that a bunch of pulses with spectrally separated positions can produce an autocorrelation trace, which resembles a single chirped

1  
2  
3 pulse autocorrelation. The traces obtained in our experiments are approximated well with the  
4  $\text{sech}^2$ -profile. If a soliton-like structure would be, indeed, represented by a bunch of  
5 conventional solitons [25, 26, 43, 44], their durations and, therefore, their energies are  
6 expected to be comparable. This is to some extent true for the autocorrelation trace observed  
7 with the InGaAs detector. However, the maximum energy of the well-developed nearly  
8 bandwidth-limited 1<sup>st</sup> Raman soliton with 195-fs duration was equal to 8 nJ, and its FWHM  
9 was 25 nm. Therefore, a pulse with 20-nJ energy and comparable duration represented by an  
10 aggregate of pulses similar to the 1<sup>st</sup> Raman soliton should reveal its internal structure in  
11 optical spectra, i.e. a few solitons should be expressed by their individual shapes in the broad  
12  $\sim 300$ -nm spectral area. Another indication of the single-pulse character of the observed  
13 soliton-like structure is that its evolution resembles the evolution of the 2<sup>nd</sup> and 3<sup>rd</sup> soliton-like  
14 pulses, which also experience spectral deformation, but tend to eventually recover their soliton  
15 spectral shape. As the deformation becomes more and more pronounced in the series of  
16 generated soliton-like pulses, it is naturally to conclude that the last pulse in the series has the  
17 same nature as the previous ones. The question of its further evolution in a longer piece of a  
18 fiber or at pump power increase is open, however.

19 The analysis of the experimental results allows us to highlight the following specific  
20 features of the pulses' evolution.

21 1. The pulse evolution is gain-driven. At low pump power, the Raman soliton resembles  
22 evolution of the conventional Raman solitons observable in long span of optical fibers. Raman  
23 soliton experiences RFSS, its spectral shape and bandwidth are preserved well. In contrast, the  
24 shape becomes gain-dependent at high pump powers. Both active medium gain and Raman  
25 gain originated from the parent pulse can contribute to the observed spectral features.

26 2. The parent pulse parameters should also affect the Raman soliton evolution. Thus,  
27 several solitons emerge at high pump powers, and the evolution of earlier born solitons  
28 stronger resembles the evolution of conventional Raman solitons. The increase in the optical  
29 gain of the active medium did not visibly impact the parameters of the 1<sup>st</sup> Raman soliton  
30 except for increase in its energy. However, when new Raman solitons appear, the state of the  
31 parent pulse (or pulses agglomerate after its break-up) is different. This change apparently  
32 dramatically affects the evolution of the newly produced Raman soliton. We anticipate that  
33 the Raman gain should play the key role in the observed changes of the pulses' evolution.

34 3. The observed pulses had a comparable duration likely originated from the mechanism  
35 of their generation. The distortion produced by subsequent amplification mainly affects their  
36 spectral broadening and chirp. Maximum pulse energy in the series of the produced pulses  
37 rises, and a new pulse becomes stronger than the previously appeared one.

38 4. The pulses formed after the generation of the 1<sup>st</sup> Raman soliton pulse and before the  
39 appearance of the last soliton-like pulse in the series tend to recover their soliton spectral  
40 shape. The stability of solitons against perturbations is well-known. The last pulse, however,  
41 did not show a RFSS, but rather an expansion in longer-wavelength domain that is likely  
42 driven by the same mechanism – Raman self-amplification. We assume that its spectral  
43 expansion occurs due to Raman amplification of its long-wavelength tail by its shorter-  
44 wavelength components. At the same time, high optical gain in the medium at these  
45 wavelengths prevents depletion of these components and compensates their extinction.  
46 Therefore, it is expected that the energy of this pulse can be further increased at higher pump  
47 powers.

48 We demonstrated that the parameters of the generated pulses can be manipulated and  
49 controlled in a wide range by a very simple means – increase of the amplifier pump power.  
50 This approach makes possible use of a simple picosecond seed laser to generate high-power  
51 femtosecond solitons with controlled spectral position or novel type of femtosecond soliton-  
52 like pulses with a very broad spectrum, which bandwidth can be also controlled. Such light  
53 sources are very attractive and promising for comb spectroscopy, which demands highly  
54 coherent spectrally broadband lasers.  
55  
56  
57  
58  
59  
60

The evolution of the seed pulse in the amplifier can be further clarified with an extension of the spectral filtering approach, which naturally occurred in our experiments due to cut-off of the semiconductor detector. More detailed fine filtering will allow to trace the pulse evolution in the spectral domain. However, this is beyond the scope of the current work.

## Conclusion

We presented experimental results on the proposed and developed Tm-doped MOPA fiber laser producing high-power ultrashort pulses with temporal  $\text{sech}^2$ -profile directly from the fiber amplifier with a low-power picosecond seed laser operating at the repetition rate of 69 MHz. The parameters of generated pulses can be easily manipulated and controlled by changing the amplifier pump power. We demonstrated the generation of a 195-fs soliton with the peak power at 30-kW level spectrally tunable in the range of  $\sim 2$ - $2.4 \mu\text{m}$ , as well as a coherent soliton-like structure with the estimated duration of 230 fs, peak power at 80-kW level, and a broad optical spectrum covering the whole range of  $1.95$ - $2.23 \mu\text{m}$  with the 3.6-dB flatness and the spectral power density  $> 3.5 \text{ mW/nm}$ . To the best of our knowledge, the latter type of pulses was observed for the first time. The maximum output power of the laser reached 3-W level.

The proposed and demonstrated approach paves the way for the generation of high-power ultrashort pulses with ultra-broad spectrum directly from a fiber amplifier with a simple picosecond seed laser. This technology is attractive and promising for the development of radiation sources for various applications, including advanced comb spectroscopy.

## Acknowledgements

This work was supported the Russian Science Foundation (Grant No. 17-72-30006).

## References

1. G. P. Agrawal, "Nonlinear fiber optics," 4th Ed., Academic Press, NY, 2007.
2. B. Bale, O. G. Okhotnikov, and S. K. Turitsyn, "Modeling and Technologies of Ultrafast Fiber Lasers," In **Fiber Lasers**, O.G. Okhotnikov (ed.), ISBN 978-3-527-41114-6 - Wiley-VCH, Berlin, 2012.
3. S. K. Turitsyn, B. Bale, and M.P. Fedoruk, "Dispersion-managed solitons in fibre systems and lasers," *Physics Reports*, **521**(4), 135-203 (2012).
4. S. Kelly, "Characteristic sideband instability of periodically amplified average soliton," *Electronics Letters*, **28**(8), 806-807 (1992).
5. E.V. Vanin, A.I. Korytin, A.M. Sergeev, D. Anderson, M. Lisak I. Vázquez, "Dissipative optical solitons," *Physical Review A* **49**(4), 2806-2811 (1994).
6. P. Grelu and N. Akhmediev, "Dissipative solitons for mode-locked lasers," *Nature Photonics*, **6**(2), 84-92 (2012).
7. A. Chong, L. G. Wright, and F. W. Wise, "Ultrafast fiber lasers based on self-similar pulse evolution: a review of current progress," *Rep. Prog. Phys.* **78**, 113901 (2015).
8. J. M. Dudley, G. Genty, S. Coen, "Supercontinuum generation in photonic crystal fiber," *Reviews of modern physics* **78**, 1135 (2006)
9. J. M. Dudley and J. R. Taylor, "Supercontinuum generation in optical fibers," Cambridge University Press, 2010.
10. A. Gelash, D. Agafontsev, V.E. Zakharov, G. El, S. Randoux, and P. Suret, "Bound State Soliton Gas Dynamics Underlying the Spontaneous Modulational Instability", *Phys. Rev. Lett.* **123**, 234102 (2019).

11. A. G. Ohkrimchuk, V. Mezentsev, V. V. Dvoyrin, A. S. Kurkov, E. M. Sholokhov, S. K. Turitsyn, A. V. Shestakov, and I. Bennion, "Waveguide-saturable absorber fabricated by femtosecond pulses in YAG:Cr<sup>4+</sup> crystal for Q-switched operation of Yb-fiber laser," *Opt. Lett.* **34**(24), 3881-3883 (2009).
12. Y. Chen, E. Rääkkönen, S. Kaasalainen, J. Suomalainen, T. Hakala, J. Hyypää, and R. Chen, "Two-channel hyperspectral LiDAR with a supercontinuum laser source," *Sensors (Basel)* **10**, 7057-7066 (2010).
13. C. Courvoisier, A. Mussot, R. Bendoula, T. Sylvestre, J. G. Reyes, G. Tribillon, B. Wacogne, T. Gharbi, H. Maillotte, "Broadband supercontinuum in a microchip-laser-pumped conventional fiber: Toward biomedical applications," *Laser Phys.* **14**, 507-514 (2004).
14. E. Sorokin "Ultrabroadband solid-state lasers in trace gas sensing," in *Mid-IR Coherent Sources and Applications*, Majid Ebrahim-Zadeh and Irina T. Sorokina, ed. (Springer, 2008, NATO science series II: Mathematics, Physics and Chemistry), 557-574.
15. F. Stutzki, C. Gaida, M. Gebhardt, F. Jansen, A. Wienke, U. Zeitner, F. Fuchs, C. Jauregui, D. Wandt, D. Kracht, J. Limpert, and A. Tünnermann, "152 W average power Tm-doped fiber CPA system," *Opt. Lett.* **39**, 4671-4674 (2014).
16. Fabian Stutzki, Christian Gaida, Martin Gebhardt, Florian Jansen, Cesar Jauregui, Jens Limpert, and Andreas Tünnermann, "Tm-based fiber-laser system with more than 200 MW peak power," *Opt. Lett.* **40**, 9-12 (2015).
17. Wan, L. Yang, and J. Liu, "High pulse energy 2  $\mu\text{m}$  femtosecond fiber laser," *Opt. Exp.* **21**, 1798-1803 (2013).
18. J. Jiang, A. Ruehl, I. Hartl and M. E. Fermann, "Coherent Tm-Fiber Raman-Soliton Amplifier," in *The European Conference on Lasers and Electro-Optics*, Technical Digest (CD) (Optical Society of America, 2011), paper CF2\_4.
19. J. Jiang, A. Ruehl, I. Hartl and M. E. Fermann, "Tunable Coherent Raman Soliton Generation with a Tm-Fiber System," in *Conference on Lasers and Electro-Optics: Science and Innovations*, Technical Digest (CD) (Optical Society of America, 2011), paper CThBB5.
20. A. S. Kurkov, V. A. Kamynin, E. M. Sholokhov, A. V. Marakulin, "Mid-IR supercontinuum generation in Ho-doped fiber amplifier," *Laser Phys. Lett.* **8**, 754-757 (2011).
21. W. Q. Yang, B. Zhang, J. Hou, R. Xiao, R. Song, and Z. J. Liu, "Gain-switched and mode-locked Tm/Ho-codoped 2  $\mu\text{m}$  fiber laser for mid-IR supercontinuum generation in a Tm-doped fiber amplifier," *Laser Phys. Lett.* **10**, 045106 (2013).
22. M. Tao, T. Yu, Z. Wang, H. Chen, Y. Shen, G. Feng, X. Ye, "Super-flat supercontinuum generation from a Tm-doped fiber amplifier," *Sci. Rep.* **6**, 23759 (2016).
23. W. Q. Yang, B. Zhang, J. Hou, R. Xiao, R. Song, Z. F. Jiang, and Z. J. Liu, "Mid-IR supercontinuum generation in Tm/Ho codoped fiber amplifier," *Laser Phys. Lett.* **10**, 055107 (2013).
24. J. Geng, Q. Wang, and S. Jiang, "High-spectral-flatness mid-infrared supercontinuum generated from a Tm-doped fiber amplifier," *Applied Optics* **51**, 834-840 (2012).
25. J. Swiderski and M. Michalska, "The generation of a broadband, spectrally flat supercontinuum extended to the mid-infrared with the use of conventional passive single-mode fibers and thulium-doped single-mode fibers pumped by 1.55  $\mu\text{m}$  pulses," *Laser Phys. Lett.* **10**, 015106 (2013).
26. J. Swiderski and M. Michalska, "Mid-infrared supercontinuum generation in a single-mode thulium-doped fiber amplifier," *Laser Phys. Lett.* **10**, 035105 (2013).
27. M. Michalska, P. Grześ, J. Swiderski, "8.76 W mid-infrared supercontinuum generation in a thulium doped fiber amplifier," *Optical Fiber Technology* **43**, 41-44 (2018).

28. K. Tarnowski, T. Martynkien, P. Mergo, J. Sotor, G. Soboń, "Compact all-fiber source of coherent linearly polarized octave-spanning supercontinuum based on normal dispersion silica fiber," *Sci. Rep.* **9**, 12313 (2019).
29. Anupamaa Rampur, Yuriy Stepanenko, Grzegorz Stępniewski, Tomasz Kardaś, Dominik Dobrakowski, Dirk-Mathys Spangenberg, Thomas Feurer, Alexander Heidt, and Mariusz Klimczak, "Ultra low-noise coherent supercontinuum amplification and compression below 100 fs in an all-fiber polarization-maintaining thulium fiber amplifier," *Opt. Express* **27**, 35041-35051 (2019).
30. Vinay V. Alexander, Zhennan Shi, Mohammed N. Islam, Kevin Ke, Michael J. Freeman, Agustin Ifarraguerri, Joseph Meola, Anthony Absi, James Leonard, Jerome Zadnik, Anthony S. Szalkowski, and Gregory J. Boer, "Power scalable >25 W supercontinuum laser from 2 to 2.5  $\mu\text{m}$  with near-diffraction-limited beam and low output variability," *Opt. Lett.* **38**, 2292-2294 (2013).
31. J. Zeng, A. E. Akosman and M. Y. Sander, "Supercontinuum Generation From a Thulium Ultrafast Fiber Laser in a High NA Silica Fiber," *IEEE Photonics Technology Letters* **31**(22), 1787-1790 (2019).
32. V. V. Dvoyrin, D. Klimentov, and I. T. Sorokina, "3W Raman Soliton Tunable between 2–2.2  $\mu\text{m}$  in Tm-Doped Fiber MOPA," in *Advanced Solid-State Lasers Congress*, M. Ebrahim-Zadeh and I. Sorokina, eds., OSA Technical Digest (online) (Optical Society of America, 2013), paper MTh1C.2.
33. I. T. Sorokina, V. V. Dvoyrin, N. Tolstik and E. Sorokin, "Mid-IR Ultrashort Pulsed Fiber-Based Lasers," *IEEE Journal of Selected Topics in Quantum Electronics* **20**(5), 99-110 (2014).
34. V. Dvoyrin and I. Sorokina, "6.8 W all-fiber supercontinuum source at 1.9-2.5  $\mu\text{m}$ ," *Laser Phys. Lett.* **11**(8), 085108 (2014).
35. D.T. Reid, W. Sibbett, J.M. Dudley, L.P. Barry, B. Thomsen, and J.D. Harvey, "Commercial Semiconductor Devices for Two Photon Absorption Autocorrelation of Ultrashort Light Pulses," *Appl. Opt.* **37**, 8142-8144 (1998).
36. I. T. Sorokina and E. Sorokin, "Femtosecond Cr<sup>2+</sup>-Based Lasers," *IEEE Journal of Selected Topics in Quantum Electronics* **21**(1), 273-291 (2015).
37. Jungkwuen An, Kyungsuk Pyun, Ojoon Kwon, and Dong Eon Kim, "An autocorrelator based on a Fabry-Perot interferometer," *Opt. Express* **21**, 70-78 (2013).
38. Shanti Toenger, Roosa Mäkitalo, Jani Ahvenjärvi, Piotr Ryzkowski, Mikko Närhi, John M. Dudley, and Goëry Genty, "Interferometric autocorrelation measurements of supercontinuum based on two-photon absorption," *J. Opt. Soc. Am. B* **36**, 1320-1326 (2019).
39. L. E. Hooper, P. J. Mosley, A. C. Muir, W. J. Wadsworth, and J. C. Knight, "Coherent supercontinuum generation in photonic crystal fiber with all-normal group velocity dispersion," *Opt. Express* **19**, 4902-4907 (2011).
40. Grzegorz Sobon, Jaroslaw Sotor, Aleksandra Przewolka, Iwona Pasternak, Wlodek Strupinski, and Krzysztof Abramski, "Amplification of noise-like pulses generated from a graphene-based Tm-doped all-fiber laser," *Opt. Express* **24**, 20359-20364 (2016).
41. K. Sala, G. Kenney-Wallace, and G. Hall, "CW autocorrelation measurements of picosecond laser pulses," *IEEE J. Quantum Electron.* **16**, 990-996 (1980).
42. C. Farrell, K. A. Serrels, T. R. Lundquist, P. Vedagarbha, and D. T. Reid, "Octave-spanning super-continuum from a silica photonic crystal fiber pumped by a 386 MHz Yb: fiber laser," *Opt. Lett.* **37**, 1778-1780 (2012).
43. C. Xia, M. Kumar, M.-Y. Cheng, O. P. Kulkarni, M. N. Islam, A. Galvanauskas, F. L. Terry Jr, M. J. Freeman, D. A. Nolan, W. A. Wood, "Supercontinuum Generation in Silica Fibers by Amplified Nanosecond Laser Diode Pulses," *IEEE Journal of Selected Topics in Quantum Electronics*, **13**(3), 789-797 (2007).

- 1  
2  
3 44. Malay Kumar, Chenan Xia, Xiuquan Ma, Vinay V. Alexander, Mohammed N. Islam,  
4 Fred L. Terry Jr, Carl C. Aleksoff, Alex Klooster, and Douglas Davidson, "Power  
5 adjustable visible supercontinuum generation using amplified nanosecond gain-switched  
6 laser diode," *Opt. Express* **16**, 6194-6201 (2008).  
7  
8  
9  
10  
11  
12  
13  
14  
15  
16  
17  
18  
19  
20  
21  
22  
23  
24  
25  
26  
27  
28  
29  
30  
31  
32  
33  
34  
35  
36  
37  
38  
39  
40  
41  
42  
43  
44  
45  
46  
47  
48  
49  
50  
51  
52  
53  
54  
55  
56  
57  
58  
59  
60

Accepted Manuscript